Single $LP_{0,n}$ mode excitation in multimode fibers

Nitin Bhatia,[1,*] **Kailash C. Rustagi,**[2] **and Joseph John**[1]

[1]*Department of Electrical Engineering, IIT-Bombay, Powai, Mumbai - 400076, India*
[2]*Department of Physics, IIT-Bombay, Powai, Mumbai - 400076, India*
[*]*nitin@ee.iitb.ac.in*

Abstract: We analyze the transmission of a Single mode - Multimode - Multimode (SMm) fiber structure with the aim of exciting a single radial mode in the second multimode fiber. We show that by appropriate choice of the length of the central multimode fiber one can obtain $> 90\%$ of the total core power in a chosen mode. We also discuss methods of removing undesirable cladding and radiation modes and estimate tolerances for practical applications.

OCIS codes: (140.3510) Lasers, fiber; (060.2320) Fiber optics amplifiers and oscillators; (060.2310) Fiber optics.

References and links

1. Y. Jeong, J. K. Sahu, D. N. Payne, and J. Nilsson, "Ytterbium-doped large-core fiber laser with 1.36 kw continuous-wave output power," Opt. Express 6088–6092 (2004).
2. J. Limpert, O. Schmidt, J. Rothhardt, F. Rser, T. Schreiber, and A. Tnnermann, "Extended single-mode photonic crystal fiber lasers," Opt. Express **14**, 2715–2720 (2006).
3. J. P. Koplow, D. A. V. Kliner, and L. Goldberg, "Single-mode operation of a coiled multimode fiber amplifier," Opt. Lett. **25**, 442–444 (2000).
4. Y. Jeong, J. K. Sahu, D. B. S. Soh, C. A. Codemard, and J. Nilsson, "High-power tunable single-frequency single-mode erbium:ytterbium codoped large-core fiber master-oscillator power amplifier source," Opt. Lett. **30**, 2997–2999 (2005).
5. P. Wang, L. J. Cooper, J. K. Sahu, and W. A. Clarkson, "Efficient single-mode operation of a cladding pumped ytterbium-doped helical-core fiber laser," Opt. Lett. **31**, 226–228 (2006).
6. J. M. Sousa and O. G. Okhotnikov, "Multimode er-doped fiber for single-transverse-mode amplification," Appl. Phys. Lett. **74**, 1528–1530 (1999).
7. X. Zhu, A. Schlzgen, H. Li, L. Li, Q. Wang, S. Suzuki, V. L. Temyanko, J. V. Moloney, and N. Peyghambarian, "Single-transverse-mode output from a fiber laser based on multimode interference," Opt. Lett. **33**, 908–910 (2008).
8. X. Zhu, A. Schlzgen, H. Li, L. Li, L. Han, J. V. Moloney, and N. Peyghambarian, "Detailed investigation of self-imaging in large core multimode optical fibers for application in fiber lasers and amplifiers," Opt. Express **16**, 16632–16645 (2008).
9. J. M. Fini and S. Ramachandran, "Natural bend-distortion immunity of higher-order-mode large-mode-area fibers," Opt. Lett. **32**, 748–750 (2007).
10. S. Ramachandran, J. W. Nicholson, S. Ghalmi, M. F. Yan, P. Wisk, E. Monberg, and F. V. Dimarcello, "Light propagation with ultralarge modal areas in optical fibers," Opt. Lett. **31**, 1797–1799 (2006).
11. Q. Wu, Y. Semenova, B. Yan, Y. Ma, P. Wang, C. Yu, and G. Farrell, "Fiber refractometer based on a fiber bragg grating and single mode - multimode - single mode fiber structure," Opt. Lett. **36**, 2197–2199 (2011).
12. J. Villatoro and D. Monzn-Hernndez, "Low-cost optical fiber refractive-index sensor based on core diameter mismatch," J. Lightwave Technol. **24**, 1409–1413 (2006).
13. O. V. Ivanov, S. A. Nikitov, and Y. V. Gulyaev, "Cladding modes of optical fibers: properties and applications," Phys. Usp. **49**, 167–191 (2006).
14. Q. Wang, G. Farrell, and W. Yan, "Investigation on single mode multimode singlemode fiber structure," J. Lightwave Technol. **26**, 512–519 (2008).

#207266 - $15.00 USD Received 26 Feb 2014; revised 9 May 2014; accepted 1 Jun 2014; published 2 Jul 2014

15. G. R. Hadley, "Wide-angle beam propagation using pade approximant operators," Opt. Lett. **17**, 1426–1428 (1992).
16. C. L. Linslal, P. M. S. Mohan, A. Halder, and T. K. Gangopadhyay, "Eigenvalue equation and core-mode cutoff of weakly guiding tapered fiber as three layer optical waveguide and used as biochemical sensor," Appl. Opt. **51**, 3445–3452 (2012).
17. *Introduction to Fiber Optics* (Cambridge University, 2011).
18. X. Zhu, A. Schulzgen, H. Li, L. Li, V. L. Temyanko, J. V. Moloney, and N. Peyghambarian, "High-power fiber lasers and amplifiers based on multimode interference," IEEE J. Sel. Top. Quantum Electron. **15**, 71–78 (2009).
19. D. Gloge, "Weakly guiding fibers," Appl. Opt. **10**, 2252–2258 (1971).
20. V. Sai, T. Kundu, C. Deshmukh, S. Titus, P. Kumar, and S. Mukherji, "Label-free fiber optic biosensor based on evanescent wave absorbance at 280nm," Sens. Actuators, B **143**, (2010).
21. R. Bharadwaj, V. Sai, K. Thakare, A. Dhawangale, T. Kundu, S. Titus, P. K. Verma, and S. Mukherji, "Evanescent wave absorbance based fiber optic biosensor for label-free detection of e. coli at 280nm wavelength," Biosens. Bioelectron. **26**, (2011).
22. X. Li, S. Lin, J. Liang, Y. Zhang, H. Oigawa, and T. Ueda, "Fiber-optic temperature sensor based on difference of thermal expansion coefficient between fused silica and metallic materials," IEEE Photon. J. **4**, 155–162 (2012).

1. Introduction

Single mode excitation of large core area fibers is attracting a lot of interest with increasing requirement of large power handling capacity of all-fiber lasers and amplifiers [1–4]. Small core single mode fibers (SMFs) can give a single transverse mode but limits the achievable power output due to non linear effects. Various techniques have been proposed for exciting a single mode in a large core area fiber such as using coiled fiber to remove the higher order modes [3], using helical core fibers, which have higher losses for higher order modes [5], designing appropriate dopant distribution to provide high gain to a single mode [6] etc. A versatile and simple way to achieve single mode beams from multimode fibers (MMFs) has also been proposed using Multimode Interference (MMI) effect [7, 8].

In this paper, we propose a method to excite a single $LP_{0,n}$ mode in the core of an MMF using Single mode - Multimode - Multimode (SMm) fiber structure shown in Fig. 1. Since a higher order mode forms a better approximation to a bessel beam, it is advantageous to excite such modes to achieve a better diffraction free beam from fiber lasers as compared to the gaussian like beam of an $LP_{0,1}$ mode. Also, bending induced mode coupling between $LP_{0,n}$ and $LP_{1,n}$ modes reduces with increasing n, due to relatively large differences between effective refractive indices of these higher order modes [9]. In yet another method, a higher order mode excitation has been achieved using a Long Period Fiber Grating (LPFG) in a fiber with specially designed refractive index profile [10]. In this method, the LPFG is used to couple the power from a single inner core mode to a higher order outer core mode of a three layered fiber structure.

The SMm structure proposed here achieves a near single mode in the core region of output MMF (MMF2) by exciting it with a specific field profile obtained by interference of propagating modes in another large core area MMF (MMF1), which in turn is excited by an SMF. Our structure is simple to fabricate and provides a novel way to excite a single $LP_{0,n}$ core mode in the standard MMFs available. Guided mode propagation analysis is employed to understand the transmission properties of this structure, and is presented in section 2. In general, with a large core area MMF1 excitation both core and cladding modes are excited in the small core area MMF2 [11–13]. In section 3, we show that with appropriate choice of the length of MMF1 a single $LP_{0,n}$ core mode can be excited in the core of MMF2. A fraction of the total power is also distributed in several cladding modes of MMF2. In section 4, we show the use of an external medium (say, a liquid or a polymer coating) surrounding MMF2 to remove the cladding modes from the structure. Section 5 discusses the use of this structure to generate a single mode beam for all-fiber lasers and amplifiers, and MMF optical sensors. In section 6, practical aspects of fabrication of the structure are presented followed by conclusions.

#207266 - $15.00 USD Received 26 Feb 2014; revised 9 May 2014; accepted 1 Jun 2014; published 2 Jul 2014

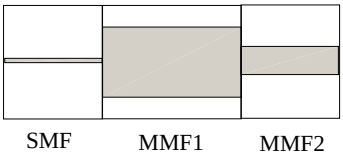

Fig. 1. Single mode - Multimode - Multimode (SMm) fiber structure (not to scale).

2. Guided mode propagation analysis of SMm

For the transmission analysis of our structure, we use core and cladding refractive indices of SMF-28 ($n_{co} = 1.4504, n_{cl} = 1.4447$) and AFS105/125Y ($n_{co} = 1.4446, n_{cl} = 1.4271$) for SMF and MMF1, respectively [14]. MMF2 is similar to MMF1, except that the core diameter is less. We used LP approximation with an assumption of infinite cladding to calculate the transverse field profiles and propagation constants of the guided core modes in fibers. The wavelength employed is $1.55\mu m$. If we assume an ideal alignment, only radial modes are excited in the structure due to symmetry [14]. Fresnel's equation is employed to calculate the average power reflection coefficient at the two junctions as

$$R = \frac{\sum_i^{N_1} \sum_j^{N_2} \mid \frac{n_i - n_j}{n_i + n_j} \mid^2}{N_1 N_2} \tag{1}$$

At the first junction (between SMF and MMF1), n_i and n_j are the effective refractive indices of the guided core modes of SMF and MMF1, respectively. At this junction, $N_1 = 1$. Similarly, at the second junction (between MMF1 and MMF2), n_i and n_j are the effective refractive indices of the guided core modes of MMF1 and MMF2, respectively. Equation 1 assumes equal power distribution in all the modes of these fibers. Using eq. 1, we get power reflection coefficients of just 0.0012% and $5.58 \times 10^{-4}\%$ at the first and the second junctions, respectively. A small reflection at the junction of SMF and MMF has already been reported in the Single mode-Multimode-Single mode (SMS) fiber structure of [14]. Reflections at the second junction can be expected to be less because the effective refractive indices of the guided modes in these MMFs are very close. Thus, we considered only the forward propagation in our analysis. Each transverse mode field is normalized to carry unity power as

$$\frac{c\varepsilon_o n}{2} \iint_A \mid \psi \mid^2 dA = 1 \tag{2}$$

where ψ is the calculated real valued mode field profile, c the velocity of light in vacuum, ε_o the permittivity of space and n the effective refractive index of the mode. At the first junction, the SMF field can be written as a linear superposition of the propagating modes of MMF1 as

$$\Phi_s = \sum_n c_n \Psi_n \tag{3}$$

where Φ_s and Ψ_n are the normalized transverse mode field profiles of the single mode fiber and the n^{th} mode of MMF1, respectively. We will show that the core modes of MMF1 are sufficient to define the input single mode field. c_n is the field coupling coefficient of the n^{th} radial mode of MMF1. It can be calculated using the orthogonality property of modes of MMF1 as

#207266 - $15.00 USD Received 26 Feb 2014; revised 9 May 2014; accepted 1 Jun 2014; published 2 Jul 2014

$$c_n = \frac{\iint_A \Phi_s \Psi_n dA}{\iint_A \Psi_n^2 dA} \tag{4}$$

This gives,

$$c_n = \sqrt{\frac{n_n}{n_s}} c'_n \tag{5}$$

where n_n and n_s are the effective refractive indices of MMF1 and SMF modes. c'_n is defined as

$$c'_n = \iint_A \frac{\phi_s}{\sqrt{\iint_A \phi_s^2 dA}} \frac{\psi_n}{\sqrt{\iint_A \psi_n^2 dA}} dA \tag{6}$$

$| c_n |^2$ gives the fraction of input power in the n^{th} radial mode of MMF1. For the above mentioned fibers, we computed field coupling coefficients and obtained $\sum_n | c_n |^2 = 0.99$. Thus, we numerically verified that the core modes of MMF1 are sufficient to describe the input SMF field. As the field propagates, individual modes develop relative phase differences between each other. The transverse field profile at any length of the MMF1 is an interference pattern of all the propagating modes. These patterns result in different power distributions on the transverse plane of the MMF1. Thus, the launch field of MMF2 depends upon the length of MMF1. This would allow the modes of MMF2 to be excited with variable power profile. To calculate the field excitation coefficients of the radial modes of MMF2, we write this launch field as

$$\sum_n c_n \Psi_n \exp(i\beta_n l) = \sum_m b_m \Psi'_m + \sum_k d_k \Psi''_k + \int p(\beta) \Psi'''_\beta d\beta \tag{7}$$

where Ψ'_m, Ψ''_k and Ψ'''_p are the transverse field profiles of the core, cladding and the radiation modes of MMF2, respectively. b_m, d_k and $p(\beta)$ are the corresponding excitation coefficients, respectively. Equation 7 is valid when the refractive index of the medium outside MMF2 is less than that of the cladding. In such a case, cladding forms a guided wave structure with the outside medium. If the refractive index of the outside medium is greater than that of the cladding, there would be leaky modes in addition to the core modes and the radiation modes in MMF2.

Using the orthogonality property of modes, the field excitation coefficients for the core modes (b_m) of MMF2 can be obtained as

$$b_m = \sum_n c_n exp(i\beta_n l) \frac{\iint_A \Psi_n \Psi'_m dA}{\iint_A \Psi'^2_m dA} \tag{8}$$

This gives,

$$b_m = \sum_n \sqrt{\frac{\alpha_m}{n_s}} c'_n a_{mn} exp(i\beta_n l) \tag{9}$$

where α_m is the effective refractive index of the m^{th} radial mode of MMF2, and a_{mn} is given by

$$a_{mn} = \iint_A \frac{\psi_n}{\sqrt{\iint_A \psi_n^2 dA}} \frac{\psi'_m}{\sqrt{\iint_A \psi'^2_m dA}} dA \tag{10}$$

#207266 - $15.00 USD Received 26 Feb 2014; revised 9 May 2014; accepted 1 Jun 2014; published 2 Jul 2014

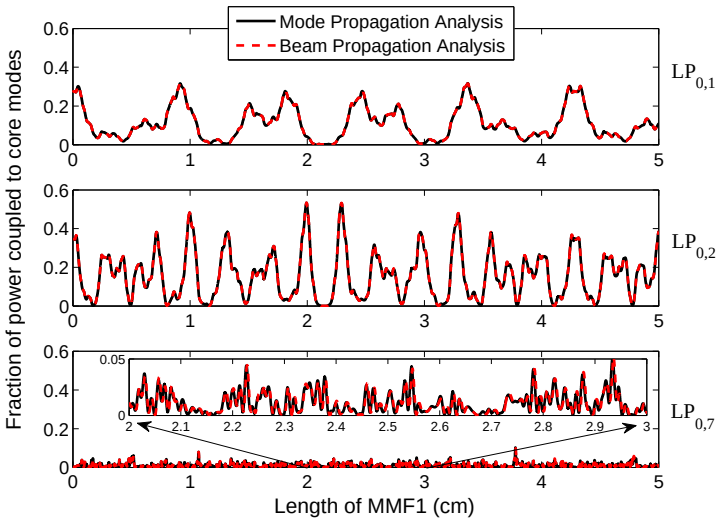

Fig. 2. Power coupled to $LP_{0,1}$, $LP_{0,2}$ and $LP_{0,7}$ modes of MMF2 for various lengths of MMF1 using two analyses. Core diameters of MMF1 and MMF2 are $50\mu m$ and $105\mu m$, respectively.

Transmission of the SMm structure for various lengths of MMF1 can be written as

$$T(dB) = 10\log_{10}(\sum_m \mid b_m \mid^2) \tag{11}$$

If the output fiber is identical to the input fiber ($m = 1$; $\alpha_1 = n_s$ and $\psi_1' = \phi_s$), eq. 11 reduces to the earlier result for the transmission of SMS structure [14]. Thus, we have a generalised form of the earlier result. Transmission through the SMm structure includes only the power coupled to the core modes of MMF2. This is because the power coupled to the cladding modes would ultimately be lost in the outer jacket or can be made to radiate away by using cladding mode strippers. To verify the above analysis, we used wide angle beam propagation method with padé order (4,4) [15], using a commercially available software package (BeamProp; Rsoft, Ver.9). We calculated the fraction of power coupled to the radial core modes ($\mid b_m \mid^2$) of a $50\mu m$ core MMF2 for different lengths of MMF1 (core $105\mu m$). Results from both the approaches are in agreement and are shown in Fig. 2 for $LP_{0,1}, LP_{0,2}$ and $LP_{0,7}$ modes of MMF2.

Transmission loss in the structure occurs because the power from MMF1 is not completely coupled to the core modes in MMF2. If $\sum_m \mid b_m \mid^2 = 1$, T = 0 dB and total power from MMF1 is coupled to MMF2 core modes. For $\sum_m \mid b_m \mid^2 < 1$, T < 0 dB and some power is coupled to the cladding/leaky modes and the radiation modes in MMF2 depending upon the refractive index contrast between cladding and the outside medium. Thus, a transmission of -3 dB would mean a transmission loss of +3 dB. To show the power coupling from MMF1 to the MMF2 cladding modes, we calculated radial mode field profiles of the cladding modes of MMF2 using three layer analysis of the fiber [16]. The refractive index of the medium outside MMF2 cladding is chosen to be 1.41. This maintains the validity of LP approximation used in calculating the modes. Field excitation coefficients of the cladding modes of MMF2 are calculated in a manner similar to that of the core modes (see eq. 9 and 10). Fraction of power coupled to the core and the cladding modes of MMF2 is shown in Fig. 3 for various lengths of MMF1. The length of MMF1 at which the fraction of power coupled to the core modes of MMF2 reaches a minimum,

#207266 - $15.00 USD Received 26 Feb 2014; revised 9 May 2014; accepted 1 Jun 2014; published 2 Jul 2014

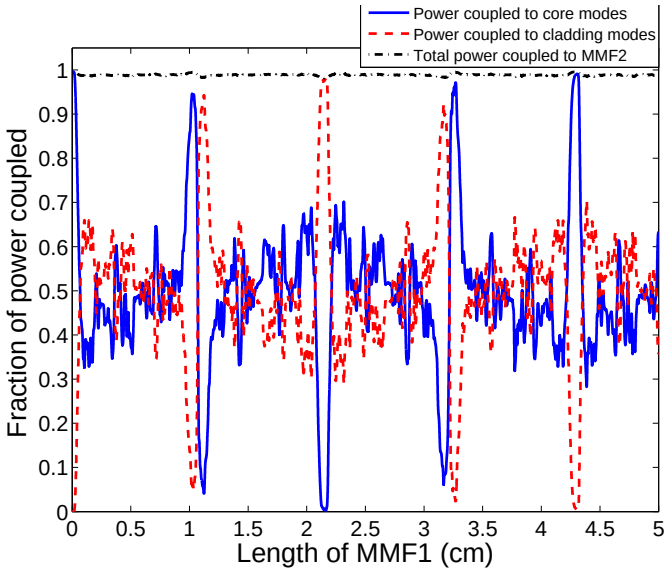

Fig. 3. Fraction of the power coupled to core ($\sum_m \mid b_m \mid^2$, solid blue line) and cladding modes ($\sum_k \mid d_k \mid^2$, dotted red line) of MMF2 as a function of the length of MMF1. Total power coupled to MMF2 ($\sum_m \mid b_m \mid^2 + \sum_k \mid d_k \mid^2$, dotted black line) is also shown.

we find that the power fraction of cladding modes reaches a maximum, and vice - versa. Figure 3 also shows that $\sum_m \mid b_m \mid^2 + \sum_k \mid d_k \mid^2 \simeq 1$. Hence, the core and cladding modes of MMF2 are sufficient to describe the MMF1 field when the refractive index of the medium surrounding MMF2 is equal to 1.41.

From the above discussion, we can conclude that for a given set of fibers, the fraction of power launched into the core and cladding modes of MMF2 can be changed by changing the length of MMF1.

3. Single $LP_{0,n}$ mode excitation in MMF2

Changing the length of MMF1 also distributes variable power amongst different core modes of MMF2. We calculated the power coupling coefficients of the radial core modes of a $50\mu m$ core MMF2 for different lengths of MMF1. Core diameter of MMF1 was chosen to be $105\mu m$. The results are shown in Fig. 4. Normalized radial power profile of the excitation field of MMF2 are also shown in the figure. Thus, it is possible to excite a set of core and cladding modes in MMF2 such that a single core mode receives a large fraction of the power coupled to all the core modes. Remaining power is coupled to the cladding modes of MMF2. Power coupled to the cladding modes can be removed by using cladding mode strippers leaving only a core mode to propagate. This technique results in the loss of power to achieve a single core mode propagation in MMF2.

To study the efficiency of this technique and to qualify the excitation of a single core mode, we put a criterion such that the desired single $LP_{0,n}$ mode in MMF2 receives more than 90% of the total power coupled to all the core modes. This condition can be written as

$$\gamma_n = \frac{\mid b_n \mid^2}{\sum_m \mid b_m \mid^2} > 0.9 \tag{12}$$

#207266 - $15.00 USD Received 26 Feb 2014; revised 9 May 2014; accepted 1 Jun 2014; published 2 Jul 2014

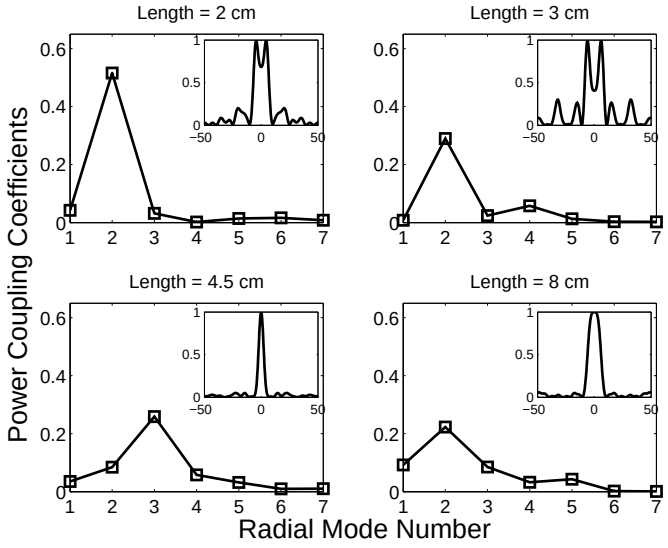

Fig. 4. Power coupling coefficients for the radial modes of a $50\mu m$ core MMF2 for different lengths of MMF1 ($105\mu m$ core) with corresponding normalized radial launch field. Dimensions of x-axis in inset is in μm.

Table 1. Fraction of power in each mode of MMF2 for different lengths and core diameters of MMF1. $LP_{0,1}$ and $LP_{0,2}$ modes are selected in MMF2.

MMF1 core	$45\mu m$		$60\mu m$	$99\mu m$
MMF2 core	$20\mu m$		$30\mu m$	
MMF1 length	$74866\mu m$	$53916\mu m$	$94938\mu m$	$10882\mu m$
$\mid b_1 \mid^2 (LP_{0,1})$	80.03%	0.02%	52.88%	0.53%
$\mid b_2 \mid^2 (LP_{0,2})$	0.09%	34.25%	1.78%	29.04%
$\mid b_3 \mid^2 (LP_{0,3})$	0.12%	0.94%	0.33%	0.20%
$\mid b_4 \mid^2 (LP_{0,4})$			0.70%	0.05%
$\mid b_5 \mid^2 (LP_{0,5})$			0.41%	0.16%
$\sum_m \mid b_m \mid^2$	80.25%	35.21%	56.10%	29.99%
Selected mode	$LP_{0,1}$	$LP_{0,2}$	$LP_{0,1}$	$LP_{0,2}$
γ_n	99.73%	97.28%	94.27%	96.83%
Loss (-T)	$0.95dB$	$4.53dB$	$2.51dB$	$5.23dB$

For various core diameters of MMF2, we calculated the lengths of MMF1 for different core diameters, that satisfies our 90% criterion. Table 1 shows the power coupling coefficients of all the radial modes of a $20\mu m$ and a $30\mu m$ core MMF2. Core diameters and the lengths of MMF1 required to achieve a single $LP_{0,1}$ or $LP_{0,2}$ core mode in these output fibers are also shown. Table also gives the fraction of power (γ_n) of the selected n^{th} radial mode of MMF2, and the corresponding transmission loss of the SMm structure.

Excitation of a higher order $LP_{0,n}$ mode requires larger core diameters of MMF2. Due to the large number of modes, the power coupled to the desired higher order mode (say, $LP_{0,10}$) of MMF2 would be less as compared to that of a smaller order mode in a small core MMF2.

#207266 - $15.00 USD Received 26 Feb 2014; revised 9 May 2014; accepted 1 Jun 2014; published 2 Jul 2014

Table 2. Selected lower and higher order radial core modes of large core diameter MMF2 for different lengths and core diameters of MMF1.

Mode	MM1 core	MMF2 core	MMF1 length	$\mid b_n \mid^2$	$\sum_m \mid b_m \mid^2$	γ_n	Loss (-T)
$LP_{0,2}$	$85\mu m$	$40\mu m$	$65314\mu m$	40.29%	41.38%	97.37%	$3.83dB$
$LP_{0,2}$	$145\mu m$	$40\mu m$	$184238\mu m$	23.77%	24.15%	98.46%	$6.17dB$
$LP_{0,3}$	$145\mu m$	$40\mu m$	$58979\mu m$	18.59%	19.60%	94.85%	$7.07dB$
$LP_{0,2}$	$86\mu m$	$50\mu m$	$125063\mu m$	49.76%	53.24%	93.46%	$2.73dB$
$LP_{0,2}$	$99\mu m$	$50\mu m$	$240728\mu m$	39.40%	40.82%	96.54%	$3.89dB$
$LP_{0,3}$	$176\mu m$	$50\mu m$	$31941\mu m$	23.03%	24.04%	95.82%	$6.19dB$
$LP_{0,10}$	$128\mu m$	$64\mu m$	$31641\mu m$	15.14%	15.53%	97.48%	$8.08dB$
$LP_{0,10}$	$174\mu m$	$64\mu m$	$57878\mu m$	09.70%	09.80%	98.96%	$10.1dB$
$LP_{0,11}$	$130\mu m$	$71\mu m$	$32637\mu m$	10.51%	10.95%	96.00%	$9.60dB$
$LP_{0,12}$	$123\mu m$	$78\mu m$	$29265\mu m$	11.25%	12.12%	92.78%	$9.16dB$
$LP_{0,22}$	$198\mu m$	$147\mu m$	$74655\mu m$	11.63%	12.42%	93.62%	$9.05dB$
$LP_{0,23}$	$199\mu m$	$154\mu m$	$75428\mu m$	10.13%	11.12%	91.17%	$9.54dB$

However, the relative power levels of these higher order modes still satisfy the 90% criterion. Table 2 shows a few design examples of exciting a higher order mode in MMF2. A value of γ as high as 0.99 is also obtained for the $LP_{0,10}$ mode in a $64\mu m$ MMF2. However, this mode is excited with only 9.7% of the input power.

4. Removal of unwanted cladding power

Since the core diameter of MMF2 is smaller than that of the MMF1, unwanted power can also propagate in the form of cladding or leaky modes in the cladding of MMF2. Normally, fibers are coated with a polymer layer with refractive index slightly higher than that of the cladding [13]. In such a case, core modes, leaky modes and radiation modes would be excited in MMF2. Relative power coupled to the leaky modes and the radiation modes depends upon the refractive index contrast of the cladding and the outside medium. Using BeamProp, we will show that a large fraction of this unwanted power (not coupled to core modes) can be removed from the structure when an outside medium with a refractive index slightly greater than that of the cladding is used. As a result, only a single core mode propagates in MMF2.

To study this effect, we removed the earlier constraint of infinite cladding medium for MMF1 and MMF2. The outside medium is assumed as air. To see the effect of limiting the cladding medium on the designed length of MMF1, we calculated the length of MMF1 to achieve maximum γ_n using BeamProp. We performed only radial calculations employing wide angle beam propagation method with padé order of (4,4) [15]. These results are presented in table 3 for all the lower order modes ($LP_{0,1}$ - $LP_{0,3}$). For all these modes, we get approximately the same length (maximum difference is of $6\mu m$) as shown in tables 1 and 2. However, the length of MMF1 to excite $LP_{0,1}$ mode in the $20\mu m$ MMF2 is quite different in the two cases. This is because the $LP_{0,1}$ mode is excited with a large amount of power for various lengths of MMF1. Even at the length of $74866\mu m$ of MMF1 (from table 1) nearly same value of $\gamma_1 (= 99.72\%)$ is obtained using BeamProp.

Now, we would like to study the effect of an outside medium surrounding MMF2, with a refractive index slightly higher than that of the cladding. For this purpose, we consider an SMm structure with MMF1 and MMF2 core diameters of $99\mu m$ and $30\mu m$, respectively. The refractive index of the medium outside MMF2 is chosen to be 1.4272. Boundaries of the simulation

#207266 - $15.00 USD Received 26 Feb 2014; revised 9 May 2014; accepted 1 Jun 2014; published 2 Jul 2014

Table 3. Length of MMF1 required to excite near single $LP_{0,n}$ mode with finite cladding diameter and outside medium as air.

Mode	MM1 core	MMF2 core	Clad Diameter	MMF1 length	γ_n
$LP_{0,1}$	$45\mu m$	$20\mu m$	$100\mu m$	$75401\mu m$	99.77%
$LP_{0,2}$	$45\mu m$	$20\mu m$	$100\mu m$	$53917\mu m$	97.20%
$LP_{0,1}$	$60\mu m$	$30\mu m$	$100\mu m$	$94938\mu m$	94.31%
$LP_{0,2}$	$99\mu m$	$30\mu m$	$125\mu m$	$10881\mu m$	96.83%
$LP_{0,2}$	$85\mu m$	$40\mu m$	$125\mu m$	$65320\mu m$	97.26%
$LP_{0,2}$	$145\mu m$	$40\mu m$	$200\mu m$	$184240\mu m$	98.49%
$LP_{0,3}$	$145\mu m$	$40\mu m$	$200\mu m$	$58980\mu m$	94.88%
$LP_{0,2}$	$86\mu m$	$50\mu m$	$125\mu m$	$125064\mu m$	93.51%
$LP_{0,2}$	$99\mu m$	$50\mu m$	$125\mu m$	$240731\mu m$	96.59%
$LP_{0,3}$	$176\mu m$	$50\mu m$	$200\mu m$	$31941\mu m$	95.82%

region were kept transparent. This enables the radiating field to escape from the simulation region, without any back reflections. Field propagating in the structure is shown in Fig. 5(a).

Figure 5(b) shows the power that would couple to the $LP_{0,2}$ mode of a $30\mu m$ core fiber, when the structure is terminated at various lengths (z). The power coupled to the $LP_{0,2}$ mode as a fraction of the input power is shown in solid green line. Similarly, the power coupled to the $LP_{0,2}$ mode as a fraction of the local propagating power is shown in dashed blue line. Total power propagating in the structure (as a fraction of input power) is also shown in dot-dashed black line. From Fig. 5(b), it can be seen that for $z < 10881\mu m$ (in MMF1), power that would couple to the $LP_{0,2}$ mode of a $30\mu m$ core fiber varies with the length of the structure. This happens due to multimode interference in MMF1. Total propagating power in MMF1 remains equal to the input power as there is no loss due to radiation. For $z > 10881\mu m$ (in MMF2), power that would couple to the $LP_{0,2}$ mode of a $30\mu m$ core fiber becomes constant. This is because MMF2 itself has a core diameter of $30\mu m$. Thus, this is the power with which $LP_{0,2}$ mode is launched in MMF2. Also, after a certain length of propagation in MMF2, total power propagating in the structure saturates nearly equal to that of the $LP_{0,2}$ core mode. This happens due to the radiation loss. As a result, power that would couple to the $LP_{0,2}$ mode, as a fraction of local propagating power, increases with the length of MMF2. This implies that the power in $LP_{0,2}$ mode of MMF2 dominates the power propagating in the structure. This power saturates at 96.78% for this design. Figure 5(b) also shows that at a length of $9131\mu m$ of MMF1, a larger fraction of the input power would be coupled to $LP_{0,2}$ mode as compared to the length of $10881\mu m$. However, this length corresponds to a lower value of $\gamma_2 (= 69.50\%)$ and is undesirable. Propagation of the $LP_{0,2}$ mode in MMF2 can be clearly seen in Fig. 5(a).

Excited higher order modes ($LP_{0,10} - LP_{0,23}$) in the SMm structure are very close to their respective cut-off conditions. The radial power profiles of $LP_{0,9}$ and $LP_{0,10}$ modes of a $64\mu m$ core fiber are shown in Fig. 6. Refractive index of the cladding is 1.4271. Thus, $LP_{0,10}$ is nearly cut-off with $n_{eff} = 1.4271043$, and carries a large amount of power in the cladding region. In contrast, the $LP_{0,9}$ mode, which is just one order less, is well confined with an effective refractive index of 1.4302373. The $LP_{0,10}$ mode has a relatively larger field amplitude at the cladding-outer medium boundary. Hence, for a smaller cladding diameter, power would leak away from this mode making it essentially leaky. This can also be seen from the effective refractive index of this mode calculated with the assumption of infinite cladding. This value is less than the refractive index of the outside medium (1.4272). Now, the effect of outside medium on the power propagating in this mode can be reduced by increasing the cladding diameter. With

#207266 - $15.00 USD Received 26 Feb 2014; revised 9 May 2014; accepted 1 Jun 2014; published 2 Jul 2014

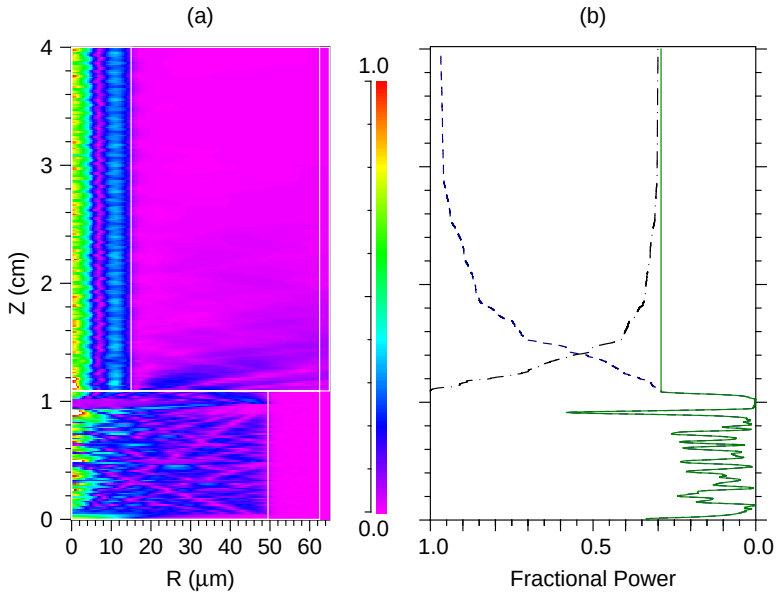

Fig. 5. (a) Propagation of field in SMm structure with MMF1 core diameter and length of $99\mu m$ and $10881\mu m$, respectively. MMF2 core diameter is $30\mu m$. Cladding diameter of MMF1 and MMF2 are $125\mu m$. MMF2 is surrounded by a medium with RI of 1.4272. This excites $LP_{0,2}$ mode in MMF2. White line shows the refractive index discontinuities in the structure. R is the length in radial direction. (b) Power that would couple to the $LP_{0,2}$ mode of a $30\mu m$ core fiber, as a fraction of local propagating power (dashed blue line) and input power (solid green line) for various lengths (z) in the structure. For $z > 10881\mu m$, this defines the propagating power in $LP_{0,2}$ mode of MMF2. Total power propagating in the structure is also shown (dot-dashed black line).

cladding diameters of $250\mu m$ and $300\mu m$, we calculated the effective refractive indices of the $LP_{0,10}$ core mode employing three layer analysis [16]. The values obtained were 1.4271035 and 1.4271039, respectively. This shows that if the diameter of cladding is increased, effective refractive index of the mode approaches the infinite cladding limit. To show this effect, we simulated our structure with different cladding diameters for the excitation of $LP_{0,10}$ mode in a $64\mu m$ MMF2. We chose the core diameter and the length of MMF1 to be $128\mu m$ and $31641\mu m$, respectively. Figure 7(a) shows the propagating field in the structure for the MMF2 cladding diameter of $150\mu m$. We can see that the $LP_{0,10}$ mode is excited at the junction of MMF1 and MMF2 but fails to propagate beyond a certain length. Figure 7(b) shows the propagation of $LP_{0,10}$ mode in the same structure but with a larger cladding diameter of $250\mu m$.

Propagation of these higher order modes can also be achieved by the use of an outside medium with a refractive index value slightly less than that of the cladding. Although, this technique allows $LP_{0,10}$ core mode to propagate without any loss but results in degradation of single mode field in MMF2 core. This happens due to propagation of the cladding modes in MMF2. Propagation of the $LP_{0,10}$ mode in MMF2 is shown in Fig. 8(a) for an outer medium having refractive index of 1.4270 surrounding MMF2. In this case, 2 cladding modes are excited in MMF2 with effective refractive indices of 1.4270996 and 1.42701813. The power coupling coefficients of these modes (calculated from eq. 9) are 14.59% and 18.28%, respectively. Fractional core (cladding + outside medium) power of these modes are 43.87% (56.12%) and

#207266 - $15.00 USD Received 26 Feb 2014; revised 9 May 2014; accepted 1 Jun 2014; published 2 Jul 2014

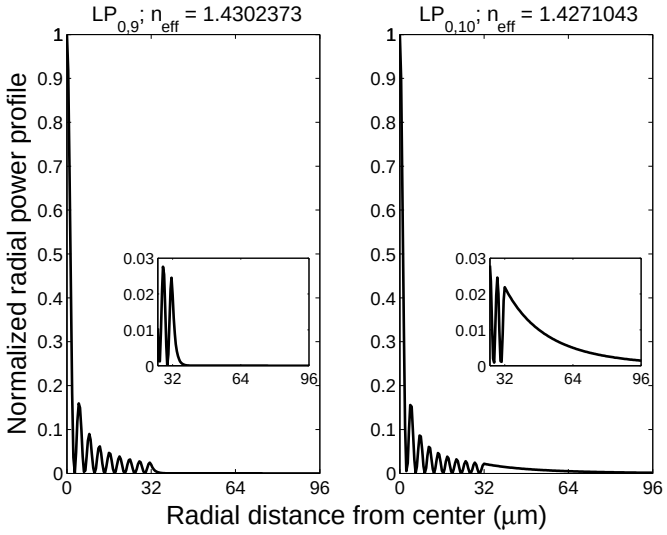

Fig. 6. Normalized radial power profile of $LP_{0,9}$ and $LP_{0,10}$ modes of $64\mu m$ core diameter fiber. $LP_{0,10}$ is near to cut-off and carry a large fraction of power in cladding. Inset shows the decaying fields of $LP_{0,9}$ and $LP_{0,10}$ modes in the cladding region.

15.77% (84.22%), respectively. The fraction of cladding mode power in the core region can be reduced by reducing the refractive index contrast between the cladding and the outside medium until the outer boundary becomes transparent. Cladding modes can be completely removed by matching the refractive index of the outside medium to that of the cladding. In such a case, neither cladding nor leaky modes are excited, and a large fraction of power would be radiated away. Propagation of the field in SMm structure for this configuration is shown in Fig. 8(b). For a small section of length of 5 cm, the medium outside MMF2 is matched with that of the cladding. In practice, this can be achieved using an index matching liquid or a polymer coating. After removal of the radiation modes in a small length of MMF2, the $LP_{0,10}$ mode propagates in the core of MMF2 with air as the medium outside cladding region.

5. Uses of SMm structure

We studied SMm structure only for a specific value of numerical aperture (0.22) of MMF1 and MMF2. Our structure gives a way to excite any desired mode in the output fiber with proper design parameters. In this section, we will discuss the use of SMm structure for exciting a single $LP_{0,n}$ mode for all-fiber lasers and amplifiers, and MMF optical sensors.

5.1. In all-fiber lasers and amplifiers

There are two different ways in which an SMm structure can be employed for all-fiber lasers. One of the techniques would be to use an active MMF1. This is in accordance with the work of Zhu *et. al.* with reference to the SMS structure [7, 8, 18]. However, with MMF1 as an active medium, different modes would see different gains depending upon their amplitudes and field profiles. This technique can affect the choice of the length of MMF1, degrade the γ factor or even lead to the loss of single mode propagation in MMF2. Thus, it would be better to filter out the mode first and then amplify it using an active medium.

Hence, we propose the use of MMF2 as an active medium for all-fiber lasers and amplifiers.

#207266 - $15.00 USD Received 26 Feb 2014; revised 9 May 2014; accepted 1 Jun 2014; published 2 Jul 2014

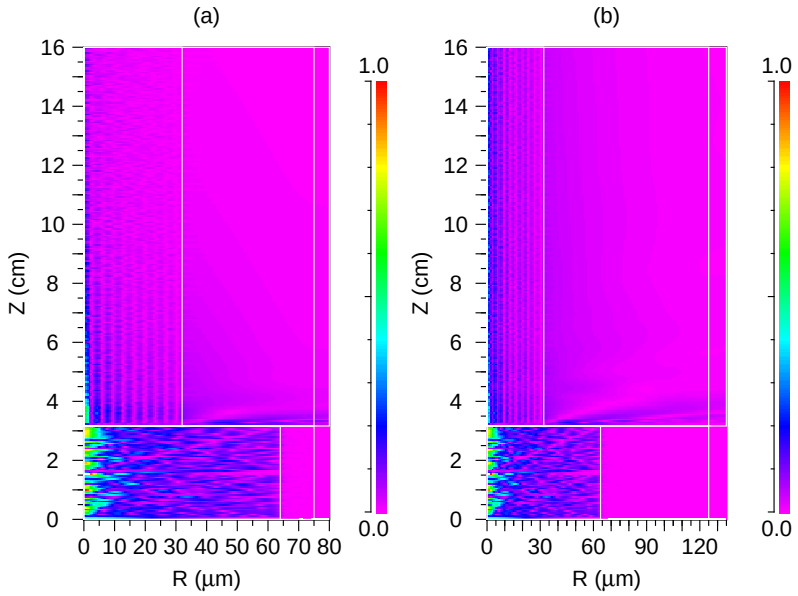

Fig. 7. Propagation of the field in SMm structure for excitation of $LP_{0,10}$ mode in MMF2. Core diameters of MMF1 and MMF2 are $128\mu m$ and $64\mu m$. RI of the medium outside MMF1 is 1.0 (air) and MMF2 is 1.4272. Cladding diameter of MMF2 in (a) is $150\mu m$ leading to leakage of power into the outer medium and in (b) is $250\mu m$ leading to propagation of the mode in the core.

An active fiber can also be spliced to MMF2 after the removal of cladding modes as depicted in Fig. 9. There is no restriction on the length of active fiber as long as mode coupling is avoided due to bending. Moreover, since a higher order mode is propagating in the core, mode coupling due to bending would be less [9]. Thus, a single higher order mode beam with very high peak intensity is possible with the structure. To demonstrate the configuration shown in Fig. 9, we excite the $LP_{0,3}$ mode in a $50\mu m$ core MMF2. The design parameters for this structure are listed in table 3. The refractive index of a small section outside the MMF2 (from 5 cm to 11 cm) is kept equal to that of the cladding. Simulation domain is terminated inside this external region with transparent boundary conditions. This configuration does not allow any reflections from the boundary of the outside medium. Figure 10 shows the results. We can see that before the matching of the cladding refractive index with that of the outside medium, the power is propagating in both the core and the cladding of MMF2. Total propagating power remains equal to the input power in MMF2. However, when the cladding refractive index is matched with that of the outside medium, the power propagating in cladding region radiates away. As a result, total propagating power reduces and saturates near to the excitation power of pure $LP_{0,3}$ mode which is now available for amplification in an active fiber. Power propagating in $LP_{0,3}$ mode as a fraction of local power saturates to 93.94%.

5.2. In optical sensing

Excited higher order modes in SMm structure are very close to their cut-off conditions. In ray optics, these modes corresponds to the rays which are launched near to the critical angle. Now, for a given V parameter, a higher order mode carries a larger amount of power in the cladding

#207266 - $15.00 USD Received 26 Feb 2014; revised 9 May 2014; accepted 1 Jun 2014; published 2 Jul 2014

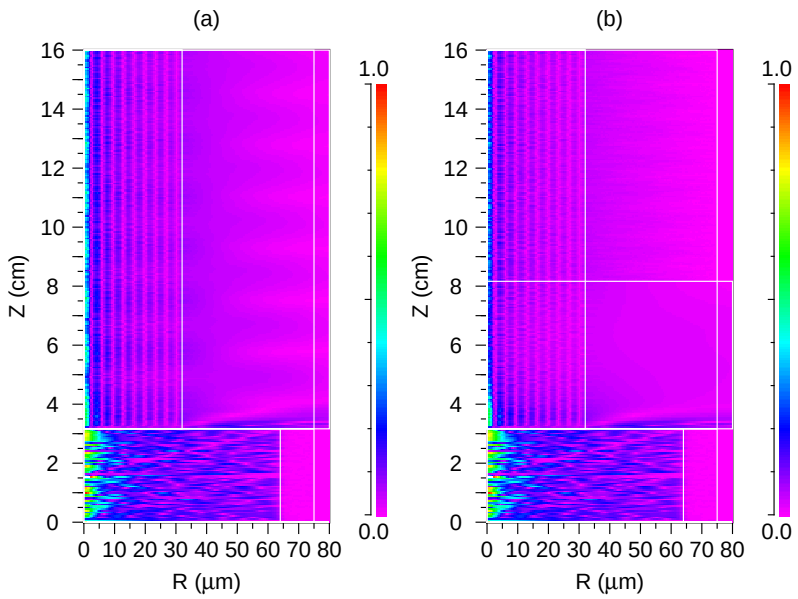

Fig. 8. Propagation of field in SMm structure for excitation of $LP_{0,10}$ mode in MMF2. Core diameters of MMF1 and MMF2 are $128\mu m$ and $64\mu m$ with cladding diameter of $150\mu m$. RI of the medium outside MMF1 is 1.0 (air). (a) shows the propagation of $LP_{0,10}$ mode in MMF2 with outer medium RI of 1.4270. (b) shows the propagation of $LP_{0,10}$ mode with outer medium RI of 1.0 (air). In this case, cladding modes are removed by exposing 5 cm of length of MMF2 ($31641\mu m - 81641\mu m$) to an outside medium with an RI value equal to that of the cladding.

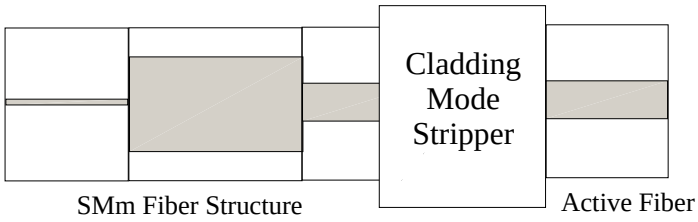

Fig. 9. Scheme to use SMm structure in high power fiber lasers and amplifiers.

#207266 - $15.00 USD Received 26 Feb 2014; revised 9 May 2014; accepted 1 Jun 2014; published 2 Jul 2014

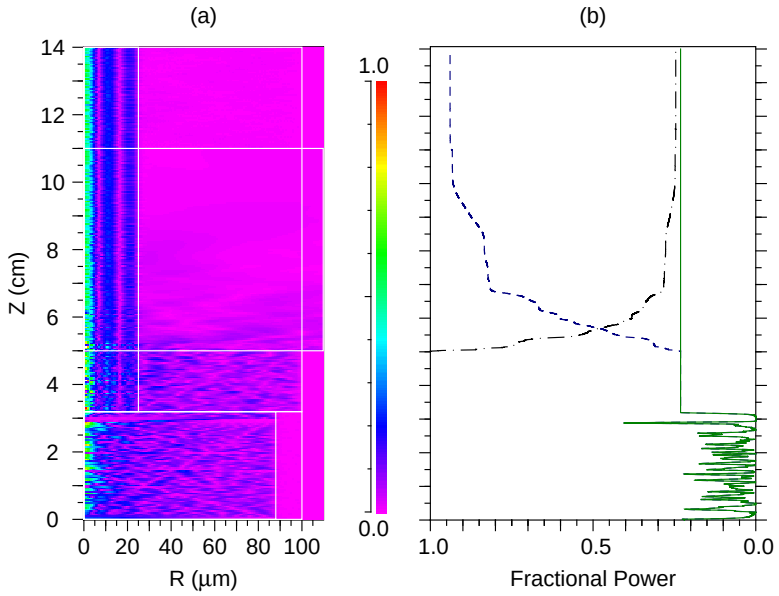

Fig. 10. BeamProp simulation of the scheme presented in Fig. 9. Core diameter of MMF1 and MMF2 are $176\mu m$ and $50\mu m$, respectively with cladding diameter of $200\mu m$. MMF1 length is $31941\mu m$. (a) When the medium outside MMF2 is air, power from MMF1 is coupled to both the core and cladding region of MMF2. Index matching liquid is applied from 5 cm - 11 cm, to radiate away this power in the cladding modes. White line shows the refractive index discontinuities in the structure. R is the length in radial direction. (b) Power that would couple to the $LP_{0,3}$ mode of a $50\mu m$ core termination fiber, as a fraction of the local propagating power (dashed line) and the input power (solid line) for various lengths (z) along the structure. For $z > 31941\mu m$, this defines the propagating power in $LP_{0,3}$ mode of MMF2. Total power propagating in the structure is also shown (dot-dashed line).

region as compared to a lower order mode [19]. Increasing power in the cladding region is beneficial for many sensing applications employing MMFs [20, 21]. For a sensor based on the absorption of evanescent power, absorbance (A) is given by [20]

$$A = \frac{P_{clad}}{P}\frac{\alpha L}{2.303} \tag{13}$$

where P_{clad} is the power in the cladding region, P the total launch power, α the absorption coefficient, and L the length of exposed fiber. P_{clad}/P naturally reduces with a large number of tightly confined propagating modes. However, for a single higher order mode propagation in MMF2, A can reach to its maximum possible value for a given MMF and enhance the sensitivity of the sensor.

6. Practical tolerances

6.1. Sensitivity to length of MMF1

Since the fraction of power coupled to the core of MMF2 depends on the length of MMF1, a good amount of accuracy would be required while splicing fibers. For all the cases presented in tables 1 and 2, we calculated the fractional power in the selected n^{th} radial mode (γ_n) near the length of its maximum value. These results for the small core MMFs presented in table 1

#207266 - $15.00 USD Received 26 Feb 2014; revised 9 May 2014; accepted 1 Jun 2014; published 2 Jul 2014

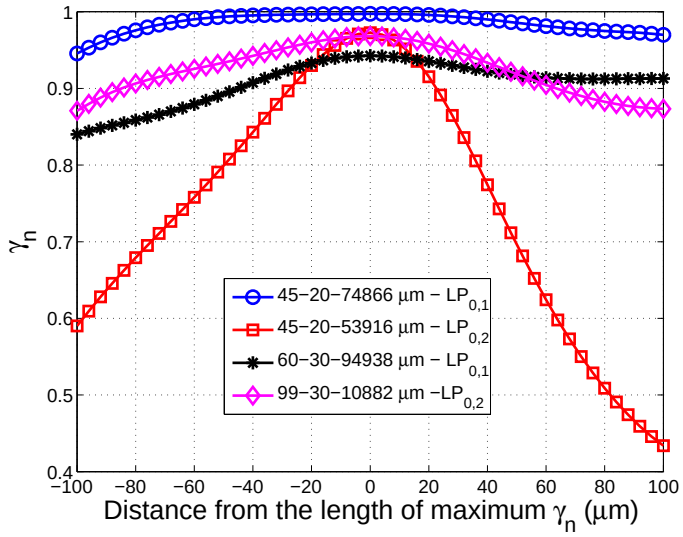

Fig. 11. Change in γ factor with change in length of MMF1 for the cases listed in table 1.

are plotted in Fig. 11. For large core fibers and higher order modes, presented in table 2, the results are plotted in Figs. 12 and 13. We observe from Figs. 11, 12 and 13 that the γ_n for higher order modes ($LP_{0,10}$ and higher) is highly immune to changes in MMF1 length. $LP_{0,1}$ and $LP_{0,2}$ modes of the $30\mu m$ core fiber also show high stability to changes in MMF1 length.

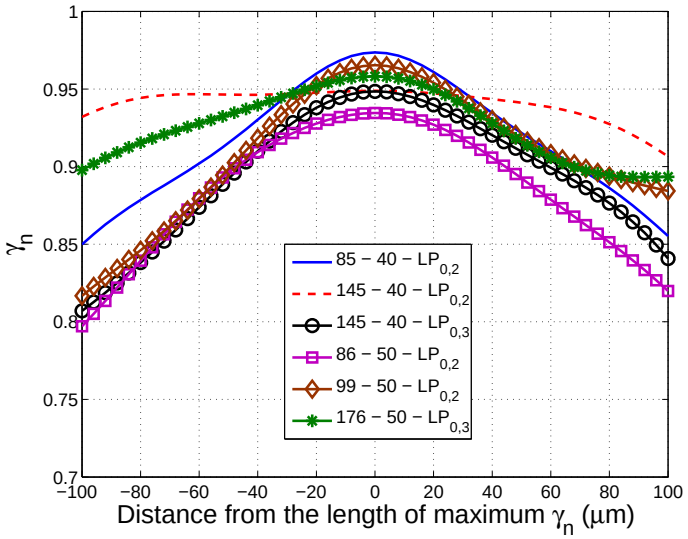

Fig. 12. Change in γ factor with change in length of MMF1 for the lower order modes ($LP_{0,2}$ and $LP_{0,3}$) presented in table 2.

#207266 - $15.00 USD Received 26 Feb 2014; revised 9 May 2014; accepted 1 Jun 2014; published 2 Jul 2014

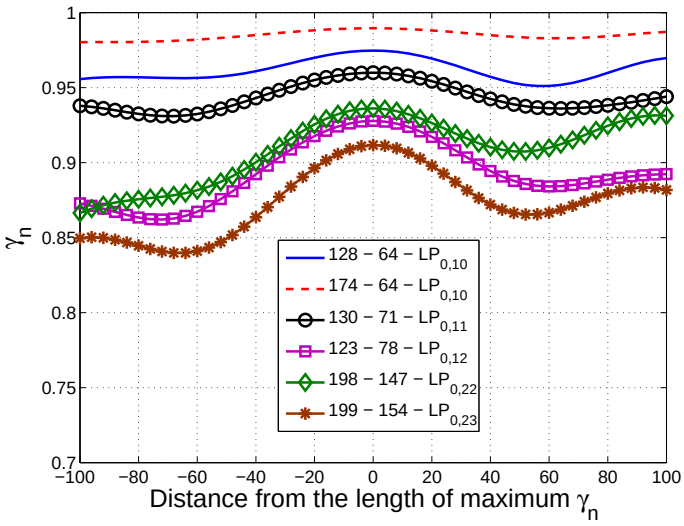

Fig. 13. Change in γ factor with change in length of MMF1 for the higher order modes ($LP_{0,10}$ - $LP_{0,23}$) presented in table 2.

6.2. Effect of temperature

Length of a fiber can also change with temperature of the surroundings. For use in fiber lasers and amplifiers, it is thus necessary to investigate the change in length of MMF1 with temperature. Coefficient of thermal expansion (α_l) of pure silica is 4×10^{-7} $/^{\circ}C$ [22]. For a small change of δT in temperature, change in the length of a fiber can be written as $\delta L = \alpha_l L \delta T$. For L = 10 cm, this corresponds to a change of 4 nm in the length per $1^{\circ}C$ change in temperature. With reference to Figs. 11, 12 and 13, we can conclude that the γ factor remains stable for a wide range of change in temperature. Also, if MMF2 is made active for use in fiber lasers and amplifiers, the junction of MMF1 and MMF2 can be sealed away in temperature controlled unit to keep the length unchanged.

7. Conclusions

Single mode - Multimode - Multimode (SMm) fiber structure provides a simple way of achieving a near single $LP_{0,n}$ core mode in standard MMFs including large core fibers. The chosen single core mode receives more than 90% of the power in the core modes. Fabrication tolerances for various designs to changes in the MMF1 lengths were also studied. The fractional power of a single $LP_{0,n}$ mode in the output fiber was observed to be highly stable. With the possibility of filtering out a single core mode, SMm forms an ideal structure to provide a seed in all-fiber laser amplifiers for achieving high intensity beams. We also suggest that the excitation of single higher order modes can be used to improve the sensitivity of fiber optic sensors based on evanescent absorption.

#207266 - $15.00 USD Received 26 Feb 2014; revised 9 May 2014; accepted 1 Jun 2014; published 2 Jul 2014